

# THE X-RAY AFTERGLOW OF THE GAMMA-RAY BURST OF 1997 MAY 8: SPECTRAL VARIABILITY AND POSSIBLE EVIDENCE OF AN IRON LINE

L. PIRO,<sup>1</sup> E. COSTA,<sup>1</sup> M. FEROCI,<sup>1</sup> F. FRONTERA,<sup>2,3</sup> L. AMATI,<sup>2</sup> D. DAL FUME,<sup>2</sup> L. A. ANTONELLI,<sup>4</sup> J. HEISE,<sup>5</sup>  
 J. IN 'T ZAND,<sup>5</sup> A. OWENS,<sup>6</sup> A. N. PARMAR,<sup>6</sup> G. CUSUMANO,<sup>7</sup> M. VIETRI,<sup>8</sup> AND G. C. PEROLA<sup>8</sup>

Received 1998 November 2; accepted 1999 January 29; published 1999 March 3

## ABSTRACT

We report the possible detection (99.3% of statistical significance) of redshifted iron line emission in the X-ray afterglow of gamma-ray burst GRB 970508 observed by *BeppoSAX*. Its energy is consistent with the redshift of the putative host galaxy determined from optical spectroscopy. The line disappeared  $\sim 1$  day after the burst. We have also analyzed the spectral variability during the outburst event that characterizes the X-ray afterglow of this gamma-ray burst. The spectrum gets harder during the flare, then becoming steep when the flux decreases. The variability, intensity, and width of the line indicate that the emitting region should have a mass  $\geq 0.5 M_{\odot}$  (assuming that the iron abundance is similar to its solar value), should have a size of  $\sim 3 \times 10^{15}$  cm, is distributed anisotropically, and is moving with subrelativistic speed. In contrast to the fairly clean environment expected in the merging of two neutron stars, the observed line properties would imply that the site of the burst is embedded in a large mass of material, consistent with preexplosion ejecta of a very massive star. This material could be related with the outburst observed in the afterglow 1 day after the GRB and with the spectral variations measured during this phase.

*Subject headings:* gamma rays: bursts — line: formation — X-rays: general

## 1. INTRODUCTION

Distance-scale determination of gamma-ray bursts (GRBs) has been one of the most important achievements of astrophysics in recent years. Accurate and fast localization of the prompt and afterglow emission bursts (i.e., Costa et al. 1997) by the Italian/Dutch X-ray satellite *BeppoSAX* (Piro, Scarsi, & Butler 1995; Boella et al. 1997) led to the identification of optical counterparts (van Paradijs et al. 1997) and ultimately to spectral measurements of a redshift (Metzger et al. 1997). While the extragalactic origin of GRBs has gathered solid evidence in its support, the source of the large energy implied by their distance is still speculative.

Direct information on the nature of the central engine of GRBs can be derived by studying the nearby environment; for example, using line spectroscopy. The star-forming region and massive preexplosion winds associated with the hypernova scenario (Paczynski 1998) imply a mass-rich environment down to short ( $\sim 10^{15}$  cm) distance scales. In contrast, neutron star–neutron star merging should happen in a fairly clean environment, because such objects are expected to form with significant speeds which can lead them at least a few parsec away from the regions of star formation in which they formed. Current line measurements are inconclusive because all of the spectral features observed so far are signatures produced by

the host galaxy rather than at the burst site. GRB 980425 is an exception, but its tantalizing association with SN 1998bw (Galama et al. 1998; Kulkarni et al. 1998) requires clarification.

The measurement of X-ray lines emitted directly by the GRB or its afterglow could provide a direct measurement of the distance and probe into the nature of the central environment (Perna & Loeb 1998). Fe K-line emission is very promising in this respect. Theoretical computations have been carried out by several authors in the framework of GRBs (Mészáros & Rees 1998; Böttcher et al. 1999; Ghisellini et al. 1999). Most of this work deals with features generated within the interstellar medium (ISM) of the host galaxy, i.e., on a scale larger than several parsec. However, even in the favorable case of dense regions of stellar formation (e.g., the site of GRB formation in the hypernova scenario), iron emission lines would be hard to detect with current X-ray instrumentation. Lately, Mészáros & Rees (1998) have shown that the circumburst environment created by the stellar wind before the explosion of the hypernova could yield a line of substantial intensity. A similarly favorable situation should be expected in a variation of the hypernova scenario, the supranova (Vietri & Stella 1998), where the GRB is shortly preceded by a supernova explosion with the ejection of an iron-rich massive shell. In these cases, and for a isotropic distribution of material around the source, a tight upper limit on the column density  $N_H < 10^{24}$  cm $^{-2}$  derives from the requirement that the Thomson optical depth be less than a few, to avoid smearing out the short timescale structure of the GRBs by Thomson scattering (Böttcher et al. 1999). Furthermore, Fe absorption features of strength comparable to that in emission should also be detected.

It is also conceivable that the impact of the relativistic shell that produced the original GRB on these ejecta could provide an additional energy input in the afterglow. GRB 970508 is the most promising candidate of the *BeppoSAX* afterglows for the search of line emission. It is characterized by a large outbursting event during its afterglow phase (Piro et al. 1998) and has the highest signal-to-noise (S/N) ratio of the *BeppoSAX* GRB afterglows. In this Letter, we present results of a spectral

<sup>1</sup> Istituto Astrofisica Spaziale, Consiglio Nazionale delle Ricerche, Via Fosso del Cavaliere 100, 00133 Rome, Italy.

<sup>2</sup> Istituto Tecnologie e Studio delle Radiazioni Extraterrestri, Consiglio Nazionale delle Ricerche, Via Gobetti 101, 40129 Bologna, Italy.

<sup>3</sup> Dipartimento di Fisica, Università Ferrara, Via Paradiso 12, Ferrara, Italy.

<sup>4</sup> *BeppoSAX* Scientific Data Center; present address: Osservatorio Astronomico di Roma.

<sup>5</sup> Space Research Organization in the Netherlands, Sorbonnelaan 2, 3584 CA Utrecht, Netherlands.

<sup>6</sup> Space Science Department of ESA, European Space Research and Technology Centre, 2200 AG Noordwijk, Netherlands.

<sup>7</sup> Istituto Fisica Cosmica e Applicazioni Calcolo Informatico, Consiglio Nazionale delle Ricerche, Via La Malfa 153, 90138 Palermo, Italy.

<sup>8</sup> Dipartimento di Fisica, Università Roma Tre, Via della Vasca Navale 84, 00146 Roma, Italy.

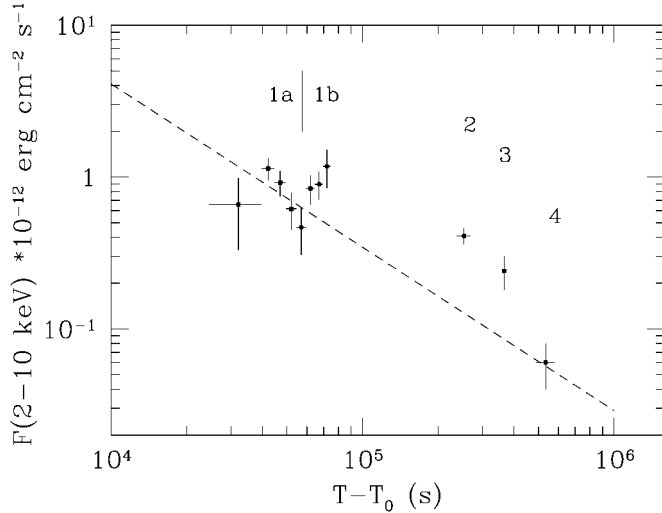


FIG. 1.—X-ray (2–10 keV) light curve of the X-ray afterglow of GRB 980508. The dashed line represents the extrapolation from the X-ray data points of the burst (Piro et al. 1998). For the spectral analysis, data from the first pointing was divided in two parts, corresponding to the transition between the decay and turn up from the light curve, creating in total five spectra (1a, 1b–4).

analysis of the afterglow of GRB 970508 and discuss their implications on the nature of the central engine of GRBs.

## 2. OBSERVATIONS OF THE X-RAY AFTERGLOW SPECTRUM OF GRB 970508

The gamma-ray burst GRB 970508 was detected by the Gamma-ray Burst Monitor aboard *BeppoSAX* (Piro et al. 1998). The Wide Field Camera provided a few arcmin position acquired with the Narrow-Field Instruments 6 hr after the burst, which led to the identification of the X-ray afterglow associated with the GRB. Three further observations were carried out, the last performed 6 days after the burst (Fig. 1, Table 1).

Low- (LECS; 0.1–3.5 keV) and medium-energy concentrator/spectrometer (MECS; 1.8–10.0 keV) spectra of the observations were obtained using standard procedures,<sup>9</sup> with 15–20 counts (source+background) per bin. Inspection of the light curve (Fig. 1) shows that in the first half period of observation number 1 the flux decays, followed by a rising trend in the

second half. We have thus split this observation into two parts (1a and 1b) at the time of the minimum of the light curve to investigate spectral evolution in different states, producing five spectra in total.

### 2.1. The Iron $K_{\alpha}$ Line

We fitted each spectrum with a power law with variable absorption, keeping the relative normalization of LECS versus MECS free to vary in the range 0.6–0.9. This model provides a good fit to all but data set 1a. In this case, we have  $\chi^2_{\nu} = 2.4$  for  $\nu = 8$  degrees of freedom, which corresponds to a probability of 1.4%.<sup>10</sup> However, the major contribution to  $\chi^2$  is not randomly distributed but is concentrated in a line feature around 3.5 keV (Fig. 2a; note that in the figure we show for clarity only data points below 2 keV for LECS and above 2 keV for MECS).

The possible association of this feature with Fe K-line emission is obvious, considering that its energy coincides with Fe I–Fe XX  $K_{\alpha}$  emission at the redshift  $z = 0.835$ , i.e., that of the putative host galaxy (Bloom et al. 1998). We have therefore added to the power-law model a narrow line (width  $\leq 1.5 \times \text{FWHM} \approx 0.5$  keV) at the energy of 3.5 keV. The relative normalization LECS/MECS that depends primarily on the position of the source in the LECS detector has, in all data sets, an error greater than the nominal range 0.6–0.9. We have hereafter fixed it to 0.8, the value averaged over all data sets. The best fit now yields  $\chi^2_{\nu} = 0.93$  with  $\nu = 7$ . The improvement of  $\Delta\chi^2/\chi^2 = 13.6$  corresponds to a confidence level of 99.3% ( $F$ -test). We stress that this confidence level relies on the a priori knowledge of the energy of the Fe line available from an independent redshift measurement. Were it not available, the confidence level for the presence of a line with free energy would have been 97%.

The best-fit line intensity is  $I_{\text{Fe}} = (5 \pm 2) \times 10^{-5}$  photons  $\text{cm}^{-2} \text{s}^{-1}$  (hereafter, all errors and upper limits correspond to 90% confidence level for a single parameter). Upper limits on line intensity in data sets 1b (Fig. 2b), 2, 3, and 4 are 2.5, 2, 2.5, and  $0.5 \times 10^{-5}$  photons  $\text{cm}^{-2} \text{s}^{-1}$ , respectively.

The power-law parameters obtained in data sets 1a and 1b are consistent with each other (see Table 1), and the absorption

<sup>10</sup> Note that GRB 970508 has the highest S/N ratio of the *BeppoSAX* GRB afterglows, so that the number of spectra with comparable statistical weight is limited to those of data set 1. We also remind the reader that the afterglow of GRB 970228 had an higher flux, but the S/N ratio was lower because data of one MECS only were usable (Costa et al. 1997).

TABLE 1  
LOG OF OBSERVATIONS AND FIT WITH A POWER LAW

| Observation              | $T_{\text{start}}^a$ | Exposure Time<br>(ks) |      | Count Rate<br>( $10^{-3}$ counts $\text{s}^{-1}$ ) |                    | $\alpha$      | $N_{\text{H}}$<br>( $10^{22} \text{ cm}^{-2}$ ) | $\chi^2/\nu$ |
|--------------------------|----------------------|-----------------------|------|--|--------------------|---------------|---|--------------|
|                          |                      | LECS                  | MECS | LECS<br>(0.1–2 keV)                                | MECS<br>(2–10 keV) |               |   |              |
| 1a <sup>b</sup> .....    | 0.24                 | 8                     | 11   | $3.0 \pm 0.8$                                      | $8.8 \pm 1.2$      | $1.5 \pm 0.9$ | $0.6^{+1.3}_{-0.55}$                            | 6.5/7        |
| 1b .....                 | 0.65                 | 7                     | 16   | $1.4 \pm 0.7$                                      | $7.2 \pm 0.9$      | $1.7 \pm 1.0$ | $1.3^{+2.5}_{-1.25}$                            | 6/9          |
| 1a+1b <sup>b</sup> ..... | 0.24                 | 15                    | 28   | $2.1 \pm 0.5$                                      | $8.3 \pm 0.8$      | $1.5 \pm 0.6$ | $0.7^{+1.5}_{-0.65}$                            | 14.2/18      |
| 2 .....                  | 2.74                 | 6                     | 24   | $1.3 \pm 0.7$                                      | $5.7 \pm 0.7$      | $0.4 \pm 0.6$ | $0.05^{+1.5}_{-0.65}$                           | 6.2/9        |
| 3 .....                  | 4.14                 | 3                     | 12   | $<1.5$   | $3.1 \pm 0.9$      | $0.5 \pm 0.8$ | 0.05 fixed                                      | 5.2/6        |
| 4 .....                  | 5.7                  | 14                    | 73   | $1.7 \pm 0.5$                                      | $1.2 \pm 0.3$      | $2.2 \pm 0.7$ | $0.05^{+0.5}$                                   | 6.3/10       |

NOTE.—Errors of spectral parameters correspond to 90% confidence level for a single parameter of interest;  $N_{\text{HGal}} = 5 \times 10^{20} \text{ cm}^{-2}$ .

<sup>a</sup> Start of the observation in days from the GRB.

<sup>b</sup> Including a line in spectral fitting of data set 1a.

<sup>9</sup> Available on the *BeppoSAX* web pages at [www.sdc.asi.it](http://www.sdc.asi.it).

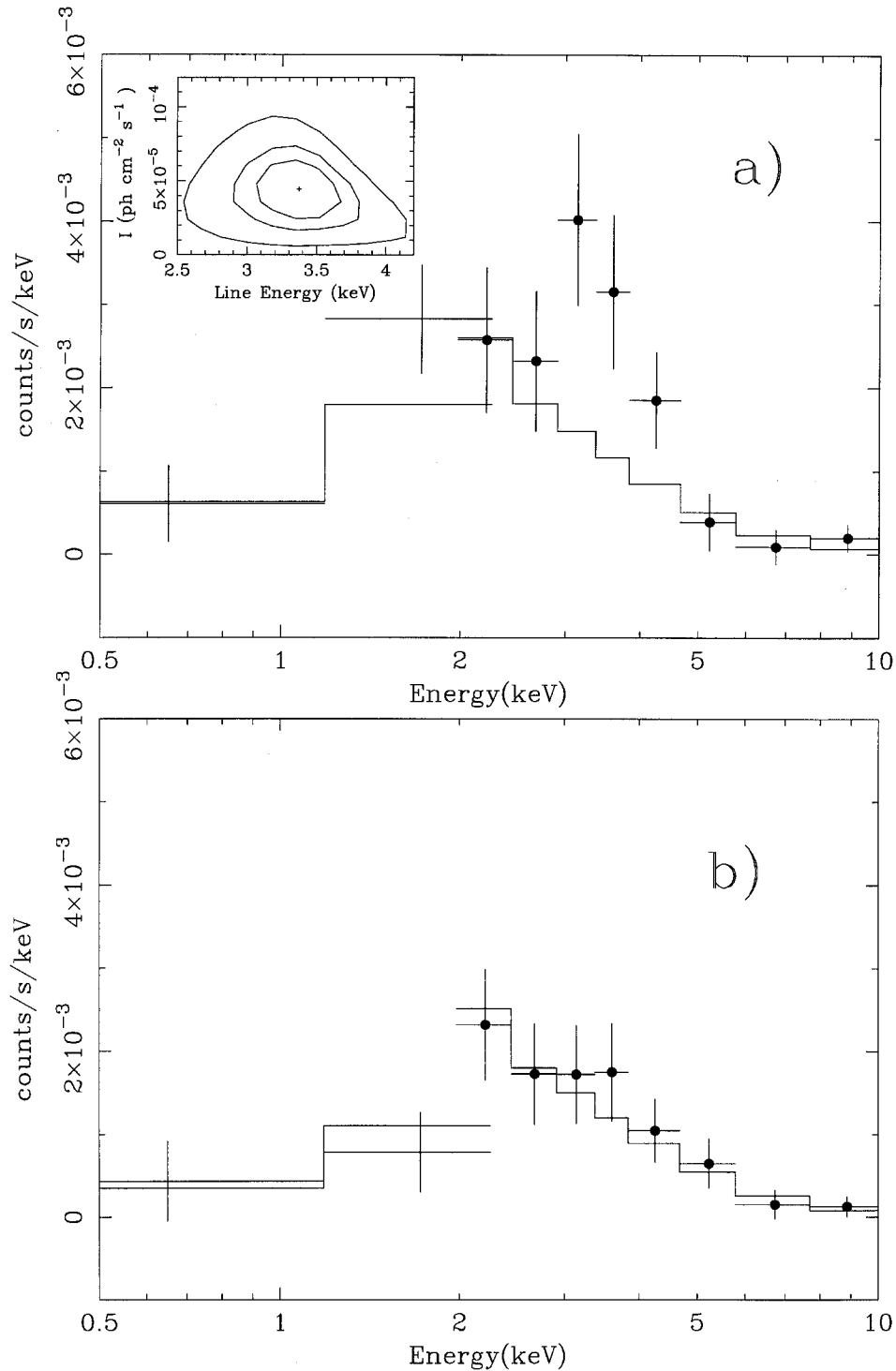


FIG. 2.—Spectra (in detector counts) of the afterglow of GRB 970508 from (a) data set 1a and (b) data set 1b. The continuous line represents the best-fit power-law continuum in the range 0.1–10 keV, excluding the interval 3–4 keV. For clarity, we show in figure LECS data below 2 keV and MECS data above 2 keV. The inset in panel *a* shows the contour plot of the line intensity vs. energy. Contours correspond to 68%, 90%, and 99% confidence levels for two interesting parameters.

column densities are consistent with the hydrogen column in the line of sight of our Galaxy, i.e., the intrinsic absorption is consistent with zero. We next performed a simultaneous fit to both data sets with the same continuum parameters and the addition of a line to data set 1a only. In this case, we left the energy of the line as free parameter, deriving  $E = 3.4 \pm 0.3$

keV, corresponding to  $6.2 \pm 0.6$  keV in the source rest frame. The error range is too large to identify the ionization state of iron. In Figure 2 (*inset*), we show the contour plot of  $I_{\text{Fe}}$  versus  $E$ .

We note that the absence of the line in data set 1b explains why a power-law model provides an acceptable fit to the

summed spectrum (Owens et al. 1998). We have also investigated whether the spectral continuum could be fitted by a blackbody or a thermal bremsstrahlung. We find that thermal models provide worse results than that of a power-law continuum, as already shown in the case of GRB 970228 (Frontera et al. 1998).

### 2.2. Spectral Variability in the Afterglow Outburst

Spectral variability of the afterglow spectra supports the idea that a refreshed energy input produced the outburst observed in the light curve. The spectral index in the first observation (Table 1) is  $\alpha = 1.5 \pm 0.6$ . In the second and third observations, the flux lies above an extrapolation of the light curve expected from a power-law evolution from the primary event. The spectrum is harder ( $\alpha = 0.4 \pm 0.6$ ), indicating electron reacceleration, as expected in a newly formed shock. In the last observation, the flux decreases and the spectrum is very steep ( $\alpha = 2.2 \pm 0.7$ ): the new energy source has been exhausted. We have noticed previously that spectra 1a and 1b are consistent with each other. Since the transition 1a–1b identifies the beginning of the outburst, one would then expect a hardening of the spectrum in 1b. However, such an effect could be masked by the continuation of the power-law decay law (Fig. 1), which accounts for about 60% of the flux observed in data set 1b.

### 3. ORIGIN OF THE LINE AND CONSTRAINTS ON THE EMITTING REGION

The minimum amount of mass  $M_{\min}$  present can be estimated (Lazzati, Campana, & Ghisellini 1999) simply by counting how many ionizing photons a given iron atom can absorb, assuming that recombination is much faster than the time interval between successive ionizations, and by demanding that the existing iron atoms thus account for the fluence in the line:

$$M_{\min} = 0.1 M_{\odot} A_{\text{Fe}}^{-1} \left( \frac{I_{\text{Fe}}}{10^{-5} \text{ photons s}^{-1} \text{ cm}^{-2}} \right) \times \frac{T}{10^5 \text{ s}} \left( \frac{R}{10^{16} \text{ cm}} \right)^2 \frac{0.1}{q} E_{52}^{-1}, \quad (1)$$

where  $A_{\text{Fe}}$  is the iron abundance in units of the solar value,  $T$  is the line duration,  $R = 10^{16} R_{16}$  cm is the distance of the medium from the central source, and  $q < 0.1$  is the fraction of the total energy  $E = 10^{52} E_{52}$  ergs that is recycled into the line. Since the line disappears after about  $10^5$  s, we expect the emitting region to have a size  $D \approx 3 \times 10^{15}$  cm; in fact, since the line width is mostly instrumental, we can bar the existence of relativistic effects. Then the typical density is  $n = 5 \times 10^9 A_{\text{Fe}}^{-1} R_{16}^2 \text{ cm}^{-3}$ , and typical Thompson and iron optical depths are  $\tau_{\text{T}} = 10 A_{\text{Fe}}^{-1} R_{16}^2$  and  $\tau_{\text{Fe}} = 5 R_{16}^2$ .

From the above, we deduce that the emitting material cannot lie along the line of sight: for  $R_{16} > 1$ ,  $\tau_{\text{T}} \gg 1$ , and Thomson scattering would smear out the time structure of the burst, contrary to observations (Böttcher et al. 1999). Even if  $A_{\text{Fe}} \gg 1$ , we would still have  $\tau_{\text{Fe}} \gg 1$ , which implies an iron edge not seen in the spectrum. For  $R_{16} < 1$ , we notice that the fireball would load itself with so many baryons as to spoil its relativistic expansion, again contradicting observations.

Having established that the emitting medium lies sideways from the line of sight, we also notice that we cannot have  $R \gg D$ , because then the line would appear much later than 1 day. We conclude that  $R \approx D$ . The ionization parameter, using

the minimum density derived above, is found to be

$$\xi = \frac{L}{nR^2} = 10^8 A_{\text{Fe}} \frac{L}{10^{50} \text{ ergs s}^{-1}} R_{16}^{-4} \approx 10^9 A_{\text{Fe}} t^{-1.1} R_{16}^{-4}, \quad (2)$$

where  $L$  is the luminosity in the range 0.016–10 keV, whose temporal evolution is approximately described by a power law (Piro et al. 1998). From equation (2), one sees that for early times ( $t \lesssim 10^4$  s), the material will be fully ionized, and thus the line may be due to recombination, while at later times, when  $\xi \lesssim 10^4$ , fluorescence may account for the emission (Kallmann & McCray 1982; Hirano et al. 1987). The exact moment of the transition cannot be determined because we established above that the emitting material lies sideways with respect to the observer, and we cannot exclude some amount of beaming, but the following discussion still stands. At early times, the emitting material will probably reach close to the inverse-Compton temperature in the burst radiation field, which clearly exceeds  $10^9$  K; for these high temperatures and low densities, recombination is not an effective emitter of line photons, and it is most likely that most of the line we see is emitted by fluorescence in the time range  $10^4 \text{ s} < t < 10^5 \text{ s}$ , during which the total observed fluence is  $\approx 10^{51}$  ergs. Putting this into equation (1), we find a minimum mass of

$$M_{\min} = 0.5 M_{\odot} A_{\text{Fe}}^{-1} \left( \frac{R_{16}}{0.3} \right)^2, \quad (3)$$

which is our best estimate for the total mass present.

### 3.1. The Site of the Line Emission

In principle, the line might arise from the normal interstellar medium surrounding the burst volume or from a normal stellar wind emitted by the burst progenitor. However, a very large density ( $n \approx 10^9 \text{ cm}^{-3}$ ) is necessary to account for the observed spectral feature; this is obvious when one considers that the line reported here is as bright as a typical one from clusters of galaxies at  $z \approx 0.1 \ll z_{970508}$ . Winds of massive stars are also unlikely to be responsible for the iron line: even for rather extreme wind parameters ( $\dot{M} = \dot{m}_{-4} \times 10^{-4} M_{\odot} \text{ yr}^{-1}$ , and  $v = v_2 \times 100 \text{ km s}^{-1}$ ), the wind density exceeds the minimum density only for  $R_{16} < 0.1 (\dot{m}_{-4} A_{\text{Fe}} / v_2)^{1/4}$ . However, for this small distance, the ionization parameter (eq. [2]) is  $\geq 10^7$  even a day after the burst and, even including beaming, the wind material will be totally ionized; under these conditions, only recombination can provide the line photons, but the recombination rates are very small ( $t_{\text{rec}} > 10^5$  s), and thus the conditions of instantaneous deexcitation under which equation (1) was established are no longer satisfied: much larger masses are required than can be accounted for by the winds. Furthermore, such small distances ( $R_{16} < 0.1$ ) cannot explain the line duration. We thus conclude that the material surrounding the burst must have been preprojected.

$A_{\text{Fe}} \approx 1$  is likely to be close to an upper limit to the iron abundance of the ISM or of a stellar wind at  $z \approx 1$ . Scenarios concerning mergers of binaries then begin to appear unlikely, regardless of whether the binary is made of two neutron stars, a black hole and a neutron star, or a black hole and a white dwarf, because it has been established (Mészáros & Rees 1992) that they cannot preject, even under the rosier assumptions, more than  $\approx 10^{-4} M_{\odot}$  due to their tidal interactions, which is about 3 orders of magnitude less than the limit in equation (1). We remark that the supranova (Vietri & Stella 1998) provides

the most appealing scenario because of the large amount of iron material ejected by the supernova explosion preceding the burst. In fact, theoretical computations of the explosion of massive stars indicate that  $\approx 0.1 M_{\odot}$  of iron are ejected by the supernova (Woosley & Weaver 1995; Thieleman, Nomoto, & Hashimoto 1996). In the case of SN 1987a, whose progenitor had  $M \approx 20 M_{\odot}$ , a similar amount of iron was derived from optical observations (Danziger & Bouchet 1993).

In the future, it is conceivable that simultaneous observations of the  $\text{Ly}\alpha$  line may help to determine  $A_{\text{Fe}}$  and thus uniquely determine the total illuminated mass, and by implication the adequacy of different formation scenarios.

#### 4. SUMMARY

In this Letter, we have obtained the following results:

1. We have searched the X-ray spectrum of GRB 970508's afterglow for an iron line, located at the system's redshift ( $z = 0.835$ ); we found such a line with limited statistical significance (99.3%) in the early part (first 16 hr) of the afterglow. The line decreases in the later part of the observations ( $\approx 1$  day after the burst) by at least a factor of 2, enough to make it undetectable with current apparatus.

2. Simultaneously with the line disappearance, the X-ray flux both rises and hardens ( $\alpha = 0.4 \pm 0.6$ , while  $\alpha = 1.5 \pm 0.6$

before the reburst), consistent with the appearance of a new shock. Then, at the end of the outburst, the spectrum steepens.

We showed that these observations indicate that a mass  $\approx 0.5 M_{\odot} A_{\text{Fe}}^{-1}$  should be located at a distance of  $3 \times 10^{15}$  cm and sideways with respect to the observer and is moving at subrelativistic speed. In order to reach such a distance, this material must have been preejected by the source originating the burst, shortly (perhaps a year, for typical supernova expansion speeds) before the burst. We stress that these observations contain two coincidences: on the one hand, this is the only burst in which a reburst and a line have been observed by *BeppoSAX*; on the other, the iron line disappears exactly at the moment of the reburst. We also point out that a line feature, with a similar significance, has been found by *ASCA* in another burst, GRB 970828, which also shows an event of rebursting during the X-ray afterglow (Yoshida et al. 1999).

We hope the report of this result will help shape future observations by X-ray satellites with superior observing capabilities, such as *XMM*, *AXAF*, and *Astro-E*.

We thank the referee, M. Böttcher, for his critical suggestions that improved the Letter substantially, F. Matteucci for helpful discussions, and the *BeppoSAX* team for support with observations. *BeppoSAX* is a program of the Italian space agency (ASI) with the participation of the Dutch space agency (NIVR).

#### REFERENCES

- Bloom, J. S., Djorgovski, S. G., Kulkarni, S. R., & Frail, D. A. 1998, *ApJ*, 507, 25
- Boella, G., Butler, R. C., Perola, G. C., Piro, L., Scarsi, L., & Bleeker, J. A. M. 1997, *A&AS*, 122, 299
- Böttcher, M., Dermer, C. D. D., Crider, A. W., & Liang, E. D. 1999, *A&A*, 343, 111
- Costa, E., et al. 1997, *Nature*, 387, 783
- Danziger, J., & Bouchet, P. 1993, in *New Aspects of Magellanic Cloud Research*, ed. B. Baschek, G. Klare, & J. Lequeux (Lecture Notes in Physics 416; Berlin: Springer), 208
- Frontera, F., et al. 1998, *ApJ*, 493, 67
- Galama, T. J., et al. 1998, *Nature*, 395, 670
- Ghisellini, G., Haardt, F., Campana, S., Lazzati, D., & Covino, S. 1999, *ApJ*, submitted (astro-ph/9808156)
- Hirano, T., Hayakawa, S., Nagase, F., Masai, K., & Mitsuda, K. 1987, *PASJ*, 39, 619
- Kallmann, T. R., & McCray, R. 1982, *ApJS*, 50, 263
- Kulkarni, S. R., et al. 1998, *Nature*, 395, 663
- Lazzati, D., Campana, S., & Ghisellini, G. 1999, *MNRAS*, in press (astro-ph/9902058)
- Mészáros, P., & Rees, M. J. 1992, *ApJ*, 397, 570
- . 1998, *MNRAS*, 299, L10
- Metzger, M. R., Djorgovski, S. G., Kulkarni, S. R., Steidel, C. C., Adelberger, K. L., Frail, D. A., Costa, E., & Frontera, F. 1997, *Nature*, 387, 878
- Owens, A., et al. 1998, *A&A*, 339, L37
- Paczynski, B. 1998, *ApJ*, 494, L45
- Perna, R., & Loeb, A. 1998, *ApJ*, 501, 467
- Piro, L., Scarsi, L., & Butler, R. C. 1995, *Proc. SPIE*, 2517, 169
- Piro, L., et al. 1998, *A&A*, 331, L41
- Thieleman, F.-K., Nomoto, K., & Hashimoto, M. 1996, *ApJ*, 460, 408
- van Paradijs, J., et al. 1997, *Nature*, 386, 686
- Vietri, M., & Stella, L. 1998, *ApJ*, 507, L45
- Woosley, S. E., & Weaver, T. A. 1995, *ApJS*, 101, 181
- Yoshida, A., et al. 1999, *A&AS*, submitted